**Title**
ELECTROSTATIC AND MAGNETOSTATIC IMAGE-FIELD COEFFICIENT



**Author**
Laslett, L. Jackson.

**Publication Date**
1969-05-01

For VII International Conference on
High-Energy Accelerators, Yerevan, USSR
August 28-Sept. 2, 1969

UCRL-18892
Preprint





# ELECTROSTATIC AND MAGNETOSTATIC IMAGE-FIELD COEFFICIENTS

L. Jackson Laslett

May 1969

AEC Contract No. W-7405-eng-48



LAWRENCE RADIATION LABORATORY
UNIVERSITY of CALIFORNIA BERKELEY

UCRL-18892

# ELECTROSTATIC AND MAGNETOSTATIC IMAGE-FIELD COEFFICIENTS*

L. Jackson Laslett

Lawrence Radiation Laboratory
University of California
Berkeley, California, U. S. A.

May 1969

## ABSTRACT

The derivation of image-field coefficients is sketched and results are presented for a particle beam centrally located within closed (elliptical or rectangular) "picture-frame" boundaries. Image-field coefficients are also given for structures that might usefully be added to a synchrotron to modify the frequencies of incoherent betatron oscillations.

Abstract for VII International Conference on High-Energy Accelerators

*Work supported by the U. S. Atomic Energy Commission.

# ELECTROSTATIC AND MAGNETOSTATIC IMAGE-FIELD COEFFICIENTS*

L. Jackson Laslett

Lawrence Radiation Laboratory
University of California
Berkeley, California, U.S.A.

June 1969

## I. INTRODUCTION

The presence of conducting or ferromagnetic boundary surfaces in the neighborhood of an intense particle beam will influence the self-fields of the beam and so affect the stability of particles in the beam. Because the analysis of such "image effects" generally requires that special treatment be given to the dc component of the magnetic field, the total space-charge force experienced by an individual particle will fail to show as rapid a decrease with energy as otherwise would be expected, and image effects accordingly play a relatively more important rôle at high energy.

Image-field coefficients have been given for several geometrical configurations in an earlier report,[1] but that work did not include examination of dc image fields for cases in which the ferromagnetic circuit completely surrounds the beam (as is the case, for example, with "picture-frame" magnets). When ferromagnetic material completely surrounds the beam, the usual condition $H_t = 0$ cannot be applied at all points on the interface, and a solution must be obtained that is consistent with the condition $\oint \vec{H}\cdot d\vec{l} = 4\pi I$.[2]

In this paper we report the derivation of electrostatic and magnetostatic image-field coefficients ($\epsilon_1$ and $\epsilon_2$, respectively, in the notation of Ref. 1) for a line beam centrally situated with respect to elliptical and rectangular boundaries. The Appendix summarizes formulas for these coefficients for several additional configurations that approximate cases of possible practical interest. The introduction of suitable boundary surfaces (such as that described for Case B2 of the Appendix) at frequent intervals around the circumference of a circular accelerator or storage ring may provide a useful passive means for reducing or suppressing space-charge effects in such a device.

## II. ELECTROSTATIC IMAGES

### 1. Elliptical Conducting Cylinder

The ellipse $(x/w)^2 + (y/h)^2 = 1$, with foci at $x = \pm f = \pm(w^2 - h^2)^{1/2}$, can be transformed [3] conformally from the $z = x + iy$ plane to the $z''$ plane by writing $z' = m \sin^{-1}(z/f)$ and $z'' = q\,\mathrm{sn}(\frac{2}{\pi}\frac{K}{m}z', k)$. The modulus $k$ of the complete elliptic integral $K$ is to be chosen so that $K'/K = (2/\pi)\tanh^{-1}(h/w)$. The electrostatic problem of a line charge $\lambda$ situated on the axis of the elliptical conducting cylinder is thereby reduced to a determination of the potential of such a charge, located at the origin, in the presence of grounded sheets that lie on the $x''$ axis in the intervals $-\infty < x'' < -q/k$, $q/k < x'' < \infty$: [4]

$$V = -2\lambda \ln\left|\frac{z'' + \sqrt{z''^2 - (q/k)^2} - iq/k}{z'' + \sqrt{z''^2 - (q/k)^2} + iq/k}\right| = -2\lambda \ln\left|\frac{k\,\mathrm{sn}(\frac{2}{\pi}K\sin^{-1}\frac{z}{f}, k)}{1 + \sqrt{1 - k^2\,\mathrm{sn}^2(\frac{2}{\pi}K\sin^{-1}\frac{z}{f}, k)}}\right| .$$

Thus, by expansion of this result through terms of order $y^2$, one obtains

$$V \doteq -2\lambda \left[\ln(\frac{kK}{\pi f}y) + \frac{2(K/\pi)^2(2 - k^2) - 1}{6}(\frac{y}{f})^2\right],$$

for the potential at a field point $z = iy$. The nonlogarithmic term within the square brackets can be identified as contributing to the image field, and the electrostatic image-field coefficient for the elliptical cylinder accordingly is given by

$$\epsilon_1 = \frac{h^2}{4\lambda}\left.\frac{\partial E_y^{\mathrm{Image}}}{\partial y}\right|_{y=0} = \frac{2(K/\pi)^2(2 - k^2) - 1}{6}\frac{h^2}{f^2} = \frac{2(K/\pi)^2(2 - k^2) - 1}{6\left[(w/h)^2 - 1\right]},$$

in agreement with a result given previously. [1]

An alternative form for the solution to the foregoing problem can be obtained by constructing a series solution for the potential problem presented in the $z'$ plane. In this plane, surfaces at $y' = \pm m \tanh^{-1}(h/w)$ are to be taken to be at zero potential, whereas the coordinate axes and vertical lines at $x' = \pm\pi m/2$ are stream lines. A series development of the potential then leads to the expression

$$\epsilon_1 = \frac{2\sum_\ell \ell\left\{1 - \tanh\left[2\ell\tanh^{-1}(h/w)\right]\right\}}{(w/h)^2 - 1},$$

a form that gives the same numerical results as the elliptic-integral expression presented above.

2. Rectangular Conducting Boundary

The image potential produced by a closed rectangular boundary ($x = \pm w$, $y = \pm h$) is reduced by the transformation $z'' = q\,\mathrm{sn}(K_1 \frac{z}{w}, k_1)$, with $K_1'/K_1 = h/w$, to the problem considered previously save that the grounded strips on the $x''$ axis now cover the intervals $-\infty < x'' < -q$ and $q < x'' < \infty$. One thus may write

$$V = -2\lambda \ln\left|\frac{z'' + \sqrt{z''^2 - q^2} - iq}{z'' + \sqrt{z''^2 - q^2} + iq}\right| = -2\lambda \ln\left|\frac{\mathrm{sn}(K\frac{z}{w}, k)}{1 + \sqrt{1 - \mathrm{sn}^2(K\frac{z}{w}, k)}}\right|$$

and

$$V \doteq -2\lambda \left[\ln(\frac{K'}{2h} y) + \frac{2k^2 - 1}{12\, h^2} K'^2\, y^2\right] \quad \text{for} \quad z = iy.$$

It then follows that

$$\epsilon_1 = \frac{2k^2 - 1}{12} K'^2 .$$

Alternatively, the rectangular boundary of course lends itself to solution of the electrostatic problem in terms of a doubly infinite array of discrete images. By this means one can obtain the result

$$\epsilon_1 = \frac{\pi^2}{48}\left[1 - (h/w)^2\right] - \frac{1}{2}\sum_{n=1}^{\infty}\sum_{m=1}^{\infty}(-1)^{n+m}\frac{n^2 - m^2w^2/h^2}{[n^2 + m^2w^2/h^2]^2}$$

$$= \frac{\pi^2}{48}\left[1 - 12\sum_{m=1}^{\infty}(-1)^{m-1}\,\mathrm{csch}\, m\pi w/h \;\; \mathrm{ctnh}\, m\pi w/h\right].$$

This last form, being rapidly convergent for small values of $h/w$, is well suited to machine computation, and leads to results in agreement with the elliptic-integral expression given in the preceding paragraph.[5]

## III. MAGNETOSTATIC IMAGES

With "picture-frame" magnets, which completely surround the particle beam, the requirement $\oint \vec{H}\cdot d\vec{l} = 4\pi I$ emu of course precludes application of the boundary condition $H_t = 0$ that normally is introduced at a ferromagnetic boundary. Instead, following a procedure described by Hague,[6] one must admit a nonvanishing tangential component of $\vec{H}$ that is continuous across the boundary, and recognize that the corresponding component of $\vec{B}$ in the ferromagnetic medium will become very large. The normal component of magnetic field, $H_n$, however, may be taken to vanish on the ferromagnetic side of the boundary (for $\mu \rightarrow \infty$), since otherwise the continuous normal component of $\vec{B}$ would become unphysically great. A solution thus can be sought such that $H_n = 0$ and $\oint H_t \, d\ell = 4\pi I$ within the ferromagnetic material. The distribution so found for $H_t$ along the interface then provides a boundary condition for solution of the interior problem -- i.e., for the vacuum region occupied by the beam.

1. Elliptical Ferromagnetic Boundary

The transformation $z' = m \sin^{-1}(z/f)$ reduces the problem of an elliptical boundary, $(x/w)^2 + (y/h)^2 = 1$, to an artificial case in which horizontal ferromagnetic boundaries are present at $y' = \pm m \tanh^{-1}(h/w)$ and in which $\vec{H}$ is normal to surfaces at $x' = \pm \pi m/2$. It is clear that a uniform field must exist within the regions occupied by ferromagnetic material in this hypothetical case and that, accordingly, the tangential magnetic field must be $\partial A_z/\partial y' = \mp 2I/m$ at the boundaries $y' = \pm m \tanh^{-1}(h/w)$. By use of the metric factor for the transformation $z'' = q \,\mathrm{sn}(\frac{2K}{\pi m} z', k)$, with $K'/K = (2/\pi) \tanh^{-1}(h/w)$, this last result is equivalent to $\frac{\partial A_z}{\partial y''} = \pm \frac{\pi I}{qK} \Big/ \sqrt{(x''^2/q^2 - 1)(k^2 x''^2/q^2 - 1)}$ above and below the $x''$ axis for $|x''| \geq q/k$. The magnetostatic vector potential is thus identical, in the $z''$ plane, to the scalar potential for a line charge ($\lambda = I$, taken to be at the origin) in the presence of an induced charge density (top plus bottom surfaces) $\sigma(x'') = -\frac{I}{2qK} \Big/ \sqrt{(x''^2/q^2 - 1)(k^2 x''^2/q^2 - 1)}$ on the surfaces $|x''| \geq q/k$, $y'' = 0$. This charge distribution contributes to the potential, at points for which $x'' = 0$, an amount

$$-2 \int_{q/k}^{\infty} \sigma(\xi) \ln(\xi^2 + y''^2) \, d\xi \quad , \quad \text{or} \quad -2 y''^2 \int_{q/k}^{\infty} \frac{\sigma(\xi)}{\xi^2} \, d\xi = \frac{I}{q^2} \left[ 1 - \frac{E}{K} \right] y''^2$$

through second order (after dropping inconsequential additive constants). One thus may write

$$A_z \doteq -2I \ln y'' + \frac{I}{q^2}\left[1 - \frac{E}{K}\right] y''^2$$

$$\doteq -2I \left\{ \ln\left(\frac{2qK}{\pi f} y\right) - \frac{1 + \left[3\left(1 - \frac{E}{K}\right) - (1 + k^2)\right]\left(\frac{2K}{\pi}\right)^2}{6 f^2} y^2 \right\} \quad \text{at} \quad x = 0,$$

from which the nonlogarithmic term gives the magnetostatic image-field coefficient

$$\varepsilon_2 \equiv \frac{h^2}{4I}\frac{\partial H_x}{\partial y} = \frac{h^2}{f^2}\,\frac{1 + \left[3\left(1 - \frac{E}{K}\right) - (1 + k^2)\right]\left(\frac{2K}{\pi}\right)^2}{6} = \frac{1 + \left[3\left(1 - \frac{E}{K}\right) - (1 + k^2)\right]\left(\frac{2K}{\pi}\right)^2}{6\left[(w/h)^2 - 1\right]}.$$

Alternatively, the artificial problem described in the $z'$ plane can be solved by constructing a formal expansion for the vector potential

$$A_z^{(\pm)} = \mp \frac{2I}{m} y' + 2I \sum_{\ell} \frac{1}{\ell}\left[\operatorname{csch}\frac{2\ell b}{m} \cosh\frac{2\ell}{m}(b \mp y') \cos\frac{2\ell}{m} x'\right] \quad (\text{for } y' \gtrless 0),$$

where $b = m \tanh^{-1}(h/w)$. By subtracting from this result the value attained in the limit $b \to \infty$ (corresponding to $h/w \to 1$), one obtains the image-field contribution from which the coefficient $\varepsilon_2$ can be derived through use of the transformation that relates $z'$ to $z$. Thus

$$\varepsilon_2 = \frac{2 \sum_{\ell} \ell \left\{\operatorname{ctnh}\left[2\ell \tanh^{-1}(h/w) - 1\right]\right\}}{(w/h)^2 - 1},$$

a result that gives the same numerical values as the elliptic-integral expression for this magnetostatic image-field coefficient. The solutions presented here permit one to plot the direction of the magnetic lines of force within an elliptical ferromagnetic cylinder by determining lines of constant $A_z$. A plot of this nature is sketched in Fig. 1 for $h/w = 0.4$, and illustrates the failure of the magnetic lines to intersect the boundary at right angles.

2. Rectangular Ferromagnetic Boundary

To obtain the magnetic boundary condition at the inner surface of a rectangular ferromagnetic yoke -- or, specifically, to obtain $H_t$ -- it is necessary first to solve the exterior problem to determine the tangential component of $\vec{H}$ within the ferromagnetic material. Bickley[7] has given a transformation that maps the exterior of the rectangle into the region exterior to a unit circle in the $t$ plane. This transformation employs elliptic functions of modulus $k$, where

$k$ is such that $\frac{h}{w} = \frac{E - k'^2 K}{E' - k^2 K'}$ and $\left|\frac{d\,\ln t}{dz}\right| = \frac{L}{h}\left|k^2 - \sin^2\theta\right|^{-1/2}$ (with $L \equiv E - k'^2 K$) for points on the boundary ($t = e^{i\theta}$). The interval $0 \leq \theta \leq \sin^{-1} k$ corresponds to the side border of the rectangle in its upper right-hand quadrant ($x = w$, $0 \leq y \leq h$), and the interval $\sin^{-1} k \leq \theta \leq \pi/2$ corresponds to the top border of this quadrant ($0 \leq x \leq w$, $y = h$). The relation between $\theta$ and the Cartesian coordinates of points on the boundary of the rectangle can be expressed in terms of incomplete elliptic integrals, but for numerical work it is convenient to employ trigonometric series with coefficients that satisfy recursion relations given by Bickley:[7]

$$x = \frac{h}{2L}\left[\cos\theta + \sum_1^\infty c_n \cos(2n-1)\theta\right],$$

$$y = \frac{h}{2L}\left[\sin\theta - \sum_1^\infty c_n \sin(2n-1)\theta\right],$$

with

$$c_{n+1} = \frac{(2n-1)^2(1-2k^2)c_n - (2n-3)(n-2)c_{n-1}}{(2n+1)(n+1)}, \quad c_o = 1, \quad c_1 = 1 - 2k^2.$$

The vector potential for the region outside the unit circle in the $t$ plane may be written $A_z = -2I\,\ln t$, and the tangential magnetic field at the boundary of the rectangle in the $z$ plane becomes

$$|H_t| = \left|\frac{dA}{dz}\right| = \left|\frac{dA}{d\,\ln t}\right| \cdot \left|\frac{d\,\ln t}{dz}\right| = 2I\,\frac{L}{h}\left|k^2 - \sin^2\theta\right|^{-1/2}.$$

The <u>image field</u>, $\vec{H}^I$, in the interior of the rectangle thus will be derivable from a vector potential $A^I$ for which $\nabla^2 A^I = 0$ at all interior points and which satisfies Neumann boundary conditions obtained by correcting the field $H_t = 2I\,\frac{L}{h}\left|k^2 - \sin^2\theta\right|^{-1/2}$ for the field produced by an isolated current $I$:

$$H_y^I = -\frac{\partial A^I}{\partial x} = 2I\left[\frac{L}{h}\frac{1}{\sqrt{k^2 - \sin^2\theta}} - \frac{w}{w^2 + y^2}\right], \qquad \text{for } x = w, \ |y| < h;$$

$$H_x^I = \frac{\partial A^I}{\partial y} = -2I\left[\frac{L}{h}\frac{1}{\sqrt{\sin^2\theta - k^2}} - \frac{h}{h^2 + x^2}\right], \qquad \text{for } y = h, \ |x| < w.$$

A harmonic series development, even in $x$ and $y$, that satisfies these boundary conditions is

$$A^{I} = \eta I (y^2 - x^2) - \frac{4I}{\pi} \sum_{m=1}^{\infty} \left[ \frac{J_m^{(1)} \cosh m\pi x/h \cos m\pi y/h}{m \sinh m\pi/\alpha} + \frac{J_m^{(2)} \cos m\pi x/w \cosh m\pi y/w}{m \sinh m\pi\alpha} \right],$$

where $\eta = \frac{\alpha}{h^2}(\gamma - \tan^{-1}\alpha)$ with $\alpha = h/w$ and $\gamma = \sin^{-1}k$,

$$J_m^{(1)} = \frac{1}{h}\int_0^h \left[ \frac{L}{\sqrt{k^2 - \sin^2\theta}} - \frac{1/\alpha}{(1/\alpha)^2 + (y/h)^2} \right] \cos m\pi y/h \, dy, \quad \text{and}$$

$$J_m^{(2)} = \frac{1}{h}\int_0^w \left[ \frac{L}{\sqrt{\sin^2\theta - k^2}} - \frac{1}{1 + (x/h)^2} \right] \cos m\pi x/w \, dx.$$

The desired magnetic image-field coefficient is then given in a form directly suitable for numerical evaluation as

$$\varepsilon_2 = \frac{\alpha}{2}(\gamma - \tan^{-1}\alpha) + \pi \sum_{m=1}^{\infty} m \left[ \frac{J_m^{(1)}}{\sinh m\pi/\alpha} - \alpha^2 \frac{J_m^{(2)}}{\sinh m\pi\alpha} \right].$$

## IV. NUMERICAL RESULTS

The results of numerical evaluation of $\varepsilon_1$ and $\varepsilon_2$, for various values of $h/w$, are listed in Tables I and II for elliptical and rectangular boundaries, respectively. Figure 2 illustrates the results graphically.

It is a pleasure to acknowledge the invaluable assistance of Mrs. Harold (Barbara) Levine in programming the LRL CDC-6600 computer for evaluation of these coefficients.

TABLE I

IMAGE-FIELD COEFFICIENTS FOR AN ELLIPTICAL BOUNDARY

| h/w | Electrostatic $\epsilon_1$ | Magnetostatic $\epsilon_2$ | h/w | Electrostatic $\epsilon_1$ | Magnetostatic $\epsilon_2$ |
|---|---|---|---|---|---|
| 0 | $\frac{\pi^2}{48} = 0.20562$ | $\frac{\pi^2}{24} = 0.41123$ | 0.50 | 0.1723 | 0.2064 |
| 0.02 | 0.2056 | 0.4014 | 0.52 | 0.1687 | 0.1991 |
| 0.04 | 0.2055 | 0.3917 | 0.54 | 0.1649 | 0.1917 |
| 0.06 | 0.2053 | 0.3823 | 0.56 | 0.1607 | 0.1843 |
| 0.08 | 0.2050 | 0.3730 | 0.58 | 0.1563 | 0.1769 |
| 0.10 | 0.2046 | 0.3640 | 0.60 | 0.1517 | 0.1694 |
| 0.12 | 0.2042 | 0.3551 | 0.62 | 0.1467 | 0.1619 |
| 0.14 | 0.2036 | 0.3464 | 0.64 | 0.1414 | 0.1544 |
| 0.16 | 0.2030 | 0.3378 | 0.66 | 0.1359 | 0.1468 |
| 0.18 | 0.2023 | 0.3294 | 0.68 | 0.1300 | 0.1391 |
| 0.20 | 0.2015 | 0.3211 | 0.70 | 0.1239 | 0.1313 |
| 0.22 | 0.2006 | 0.3129 | 0.72 | 0.1174 | 0.1235 |
| 0.24 | 0.1996 | 0.3049 | 0.74 | 0.1107 | 0.1156 |
| 0.26 | 0.1984 | 0.2969 | 0.76 | 0.1037 | 0.1075 |
| 0.28 | 0.1972 | 0.2890 | 0.78 | 0.09647 | 0.09937 |
| 0.30 | 0.1958 | 0.2812 | 0.80 | 0.08893 | 0.09110 |
| 0.32 | 0.1943 | 0.2735 | 0.82 | 0.08112 | 0.08269 |
| 0.34 | 0.1926 | 0.2659 | 0.84 | 0.07306 | 0.07415 |
| 0.36 | 0.1907 | 0.2584 | 0.86 | 0.06474 | 0.06547 |
| 0.38 | 0.1887 | 0.2508 | 0.88 | 0.05617 | 0.05663 |
| 0.40 | 0.1865 | 0.2434 | 0.90 | 0.04737 | 0.04763 |
| 0.42 | 0.1841 | 0.2359 | 0.92 | 0.03833 | 0.03847 |
| 0.44 | 0.1815 | 0.2285 | 0.94 | 0.02907 | 0.02913 |
| 0.46 | 0.1787 | 0.2212 | 0.96 | 0.01959 | 0.01961 |
| 0.48 | 0.1756 | 0.2138 | 0.98 | 0.00990 | 0.00990 |
| | | | 1.00 | 0 | 0 |

TABLE II

IMAGE-FIELD COEFFICIENTS FOR A RECTANGULAR BOUNDARY

| h/w | Electrostatic $\varepsilon_1$ | Magnetostatic $\varepsilon_2$ | h/w | Electrostatic $\varepsilon_1$ | Magnetostatic $\varepsilon_2$ |
|---|---|---|---|---|---|
| 0 | $\frac{\pi^2}{48} = 0.20562$ | | | | |
| 0.18 | 0.2056 | | | | |
| 0.20 | 0.2056 | 0.329 | 0.60 | 0.1795 | 0.189 |
| 0.22 | 0.2056 | 0.321 | 0.62 | 0.1747 | 0.181 |
| 0.24 | 0.2056 | 0.314 | 0.64 | 0.1694 | 0.173 |
| 0.26 | 0.2056 | 0.307 | 0.66 | 0.1637 | 0.165 |
| 0.28 | 0.2055 | 0.301 | 0.68 | 0.1575 | 0.157 |
| 0.30 | 0.2055 | 0.294 | 0.70 | 0.1507 | 0.149 |
| 0.32 | 0.2053 | 0.287 | 0.72 | 0.1435 | 0.140 |
| 0.34 | 0.2051 | 0.280 | 0.74 | 0.1359 | 0.132 |
| 0.36 | 0.2048 | 0.273 | 0.76 | 0.1277 | 0.123 |
| 0.38 | 0.2043 | 0.266 | 0.78 | 0.1192 | 0.114 |
| 0.40 | 0.2037 | 0.260 | 0.80 | 0.1101 | 0.104 |
| 0.42 | 0.2028 | 0.253 | 0.82 | 0.1007 | 0.095 |
| 0.44 | 0.2017 | 0.246 | 0.84 | 0.09092 | 0.085 |
| 0.46 | 0.2003 | 0.239 | 0.86 | 0.08071 | 0.075 |
| 0.48 | 0.1985 | 0.232 | 0.88 | 0.07015 | 0.065 |
| 0.50 | 0.1964 | 0.225 | 0.90 | 0.05923 | 0.055 |
| 0.52 | 0.1939 | 0.218 | 0.92 | 0.04798 | 0.044 |
| 0.54 | 0.1910 | 0.211 | 0.94 | 0.03642 | 0.034 |
| 0.56 | 0.1876 | 0.204 | 0.96 | 0.02456 | 0.023 |
| 0.58 | 0.1838 | 0.197 | 0.98 | 0.01241 | 0.011 |
| | | | 1.00 | 0 | 0 |

## APPENDIX

The following summary presents expressions for the incoherent electrostatic and magnetostatic image-field coefficients, $\varepsilon_1$ and $\varepsilon_2$, for several boundary configurations. Because the image fields are such that $\vec{\nabla}\cdot\vec{E}^{(I)} = 0$ and $\vec{\nabla}\times\vec{B}^{(I)} = 0$, the effect of these fields on the frequencies of betatron oscillation normally will be such that $Q_y^2$ and $Q_x^2$ will change by the same amount in opposite directions. In case the changes introduced in the boundary configuration are of a period similar to that of an existing alternating-gradient focusing field, however, the influence of these changes may be significantly different from that expected in a constant-gradient structure and a specific dynamical analysis will then be required.

In each of the following cases, the line beam ($\lambda$, I) is considered to be centrally located with respect to the structure (at $|z| = 0$), and expressions for the image effects are for $|z|$ small. The half-height and the half-width of the boundary are respectively denoted by h and w. The image-field coefficients are defined as follows in terms of the image fields:

$$\frac{1}{\lambda}\frac{\partial E_y}{\partial y} = -\frac{1}{\lambda}\frac{\partial E_x}{\partial x} = 4\frac{\varepsilon_1}{h^2} = 4\frac{\varepsilon_1'}{w^2};$$

$$\frac{1}{I}\frac{\partial H_x}{\partial y} = \frac{1}{I}\frac{\partial H_y}{\partial x} = 4\frac{\varepsilon_2}{h^2} = 4\frac{\varepsilon_2'}{w^2}.$$

A. <u>Electrostatic Coefficients</u>

1a. Infinite Horizontal Conducting Plates, at $y = \pm h$: [1]

$$V = -2\lambda \ln\left|\tanh\frac{\pi z}{4h}\right|,$$

$$V^{(I)} \cong \frac{\pi^2}{24}\frac{x^2 - y^2}{h^2}\lambda,$$

$$\varepsilon_1 = \frac{\pi^2}{48} \doteq 0.20562$$

1b. Infinite Vertical Conducting Plates, at $x = \pm w$:

$$\varepsilon_1' = -\frac{\pi^2}{48} \doteq -0.20562$$

2. Elliptical Conducting Tube; vertical semi-axis = h, horizontal semi-axis = w, $f = (w^2 - h^2)^{1/2}$:

$$V = -2\lambda \ln \left| \frac{k\,\mathrm{sn}(\frac{2}{\pi} K \sin^{-1}\frac{z}{f},\, k)}{1 + \sqrt{1 - k^2\,\mathrm{sn}^2(\frac{2}{\pi} K \sin^{-1}\frac{z}{f},\, k)}} \right| ,$$

where (Sect. II,1)

$$K'/K = (2/\pi)\tanh^{-1}(h/w) ;$$

$$V^{(I)} \cong \frac{2(K/\pi)^2(2-k^2) - 1}{3}\,\frac{x^2 - y^2}{f^2}\lambda ,$$

$$\epsilon_1 = \frac{2(K/\pi)^2(2-k^2) - 1}{6\left[(w/h)^2 - 1\right]} , \qquad \epsilon_1' = \frac{2(K/\pi)^2(2-k^2) - 1}{6\left[1 - (h/w)^2\right]} .$$

3. Rectangular Conducting Box; half-height = h, half-width = w:

$$V = -2\lambda \ln \left| \frac{\mathrm{sn}(K\frac{z}{w},\, k)}{1 + \sqrt{1 - \mathrm{sn}^2(K\frac{z}{w},\, k)}} \right| ,$$

where (Sect. II,2)

$$K'/K = h/w ;$$

$$V^{(I)} \cong \frac{2k^2 - 1}{6} K^2 \frac{x^2 - y^2}{w^2}\lambda ,$$

$$\epsilon_1 = \frac{2k^2 - 1}{12} K'^2 , \qquad \epsilon_1' = \frac{2k^2 - 1}{12} K^2 .$$

4. Infinite Horizontal Conducting Strips, at $|x| \geq w$, $y = 0$:

$$V = -2\lambda \ln \left| \frac{z/w}{1 + \sqrt{1 - (z/w)^2}} \right| ,$$

$$V^{(I)} \cong -\frac{x^2 - y^2}{2w^2}\lambda ,$$

$$\epsilon_1' = -\frac{1}{4} .$$

5. Hyperbolic Conducting Cylinders, $\dfrac{x^2}{w^2} - \dfrac{y^2}{f^2 - w^2} = 1$:

$$V = -2\lambda \ln \left| \tan\left(\frac{\pi}{4}\,\frac{\sin^{-1} z/f}{\sin^{-1} w/f}\right) \right| ,$$

$$V^{(I)} \cong -\left[1 + \frac{\pi^2}{8(\sin^{-1}\frac{w}{f})^2}\right] \frac{x^2 - y^2}{3f^2}\lambda ,$$

$$\epsilon_1' = -\frac{1}{6}\left[1 + \frac{\pi^2}{8(\sin^{-1}\frac{w}{f})^2}\right]\left(\frac{w}{f}\right)^2 ,$$

for which $\epsilon_1' \to -1/4$ as $w/f \to 1$ (as found for Case A5) and $\epsilon_1' \to -\pi^2/48$ as $f \to \infty$ (as found for Case A1b).

B. Magnetostatic Coefficients

1a. Infinite Horizontal Ferromagnetic Pole Surfaces, at $y = \pm h$: [1]

$$A = -2I \ln\left|\sinh \frac{\pi}{2}\frac{z}{h}\right| ,$$

$$A^{(I)} \cong -\frac{\pi^2}{12}\frac{x^2 - y^2}{h^2} I ,$$

$$\varepsilon_2 = \frac{\pi^2}{24} \doteq 0.41123$$

1b. Infinite Vertical Ferromagnetic Pole Surfaces, at $x = \pm w$:

$$\varepsilon_2' = -\frac{\pi^2}{24} \doteq -0.41123$$

2. Elliptical Ferromagnetic box -- with vertical semi-axis = h, horizontal semi-axis = w -- with slits above and below the beam:

$$A = -2I \ln\left|\operatorname{sn}\left(\frac{2K}{\pi}\sin^{-1}\frac{z}{\sqrt{w^2 - h^2}}, k\right)\right| ,$$

where

$$K'/K = (2/\pi)\tanh^{-1}(h/w) ;$$

$$A^{(I)} \cong \frac{4(K/\pi)^2(k^2+1) - 1}{3}\frac{x^2 - y^2}{w^2 - h^2} I ,$$

$$\varepsilon_2 = -\frac{4(K/\pi)^2(k^2+1) - 1}{6}\frac{h^2}{w^2 - h^2} ,$$

$$\varepsilon_2' = -\frac{4(K/\pi)^2(k^2+1) - 1}{6}\frac{w^2}{w^2 - h^2} ,$$

for which $\varepsilon_2 \to -\pi^2/12 \doteq -0.8225$ as $h/w \to 0$ and $\varepsilon_2 \to -1$ as $h/w \to 1$.

3. Rectangular Ferromagnetic box -- of half-height = h, half-width = w -- with slits above and below the beam:

$$A = -2I \ln\left|\operatorname{sn}\left(K\frac{z}{w}, k\right)\right| ,$$

where

$$K'/K = h/w ;$$

$$A^{(I)} \cong \frac{k^2+1}{3} K^2 \frac{x^2 - y^2}{w^2} I ,$$

$$\varepsilon_2 = -\frac{k^2+1}{6} K'^2 , \qquad \varepsilon_2' = -\frac{k^2+1}{6} K^2 ,$$

for which $\varepsilon_2 = -\pi^2/12 \doteq -0.8225$ for $h/w = 0$,

$\varepsilon_2 = \varepsilon_2' \doteq -0.8594$ for $h/w = 1$, and

$\varepsilon_2' \to -\pi^2/24 \doteq -0.4112$ as $h/w \to \infty$ (as found for Case B1b).

4. Horizontal Thin Passive Ferromagnetic Strips, at $|x| \geq w$, $y = 0$:

Horizontal strips of magnetic material, if infinitely thin and in a plane that contains the beam current, do not interfere with the magnetic flux lines; accordingly

$$\epsilon_2' = 0$$

in this situation.

5. Hyperbolic Ferromagnetic Cylinders, $\frac{x^2}{w^2} - \frac{y^2}{f^2 - w^2} = 1$:

$$A = -2I \ln \left| \sin\left(\frac{\pi}{2} \frac{\sin^{-1} \frac{z}{f}}{\sin^{-1} \frac{w}{f}}\right) \right| ,$$

$$A^{(I)} \cong \left[ \frac{\pi^2}{4(\sin^{-1} \frac{w}{f})^2} - 1 \right] \frac{x^2 - y^2}{3f^2} I ,$$

$$\epsilon_2' = -\frac{1}{6} \left[ \frac{\pi^2}{4(\sin^{-1} \frac{w}{f})^2} - 1 \right] \left(\frac{w}{f}\right)^2 ,$$

for which $\epsilon_2' = 0$ for $w = f$ (as in Case B4) and $\epsilon_2' \to -\pi^2/24 \doteq -0.41123$ as $f \to \infty$ (as found for Case B1b).

REFERENCES:

*Work supported by the U.S. Atomic Energy Commission.

[1] L. Jackson Laslett, in Proceedings of the 1963 Summer Study on Storage Rings, Accelerators and Experimentation at Super-High Energies (J. W. Bittner, ed.), BNL-7534, pp. 324 - 367 (Brookhaven Natl. Lab., Upton, New York, 1963).

[2] Ref. 1, p. 351.

[3] Ref. 1, p. 358.

[4] W. R. Smythe, Static and Dynamic Electricity (McGraw-Hill Book Co., New York, 1939), Ed. 1, Problem 32, p. 104, with d = 0.

[5] The sum of terms that a doubly infinite array of alternating line charges contributes to the electrostatic potential can be reduced in this case to the elliptic-integral result -- see W. H. Hicks, Q. J. Pure Appl. Math. 15 274 - 315 (1878), esp. Sects. 17 - 19, pp. 293 - 296.

[6] B. Hague, The Principles of Electromagnetism Applied to Electrical Machines (Dover, New York, 1962) -- previously Electromagnetic Problems in Electrical Engineering (Oxford University Press, 1929).

[7] W. G. Bickley, Proc. London Math. Soc. (2) 37, 82 - 105 (March, 1934), esp. pp. 83 - 91.

CAPTIONS FOR FIGURES:

FIG. 1. Lines of constant vector potential, indicating the direction of the magnetic field due to a centrally located line current within an elliptical ferromagnetic cylinder with $h/w = 0.4$ (only one quadrant shown).

FIG. 2. Electrostatic and magnetostatic image-field coefficients ($\epsilon_1$ and $\epsilon_2$) for elliptical and rectangular boundaries, vs. $h/w$.

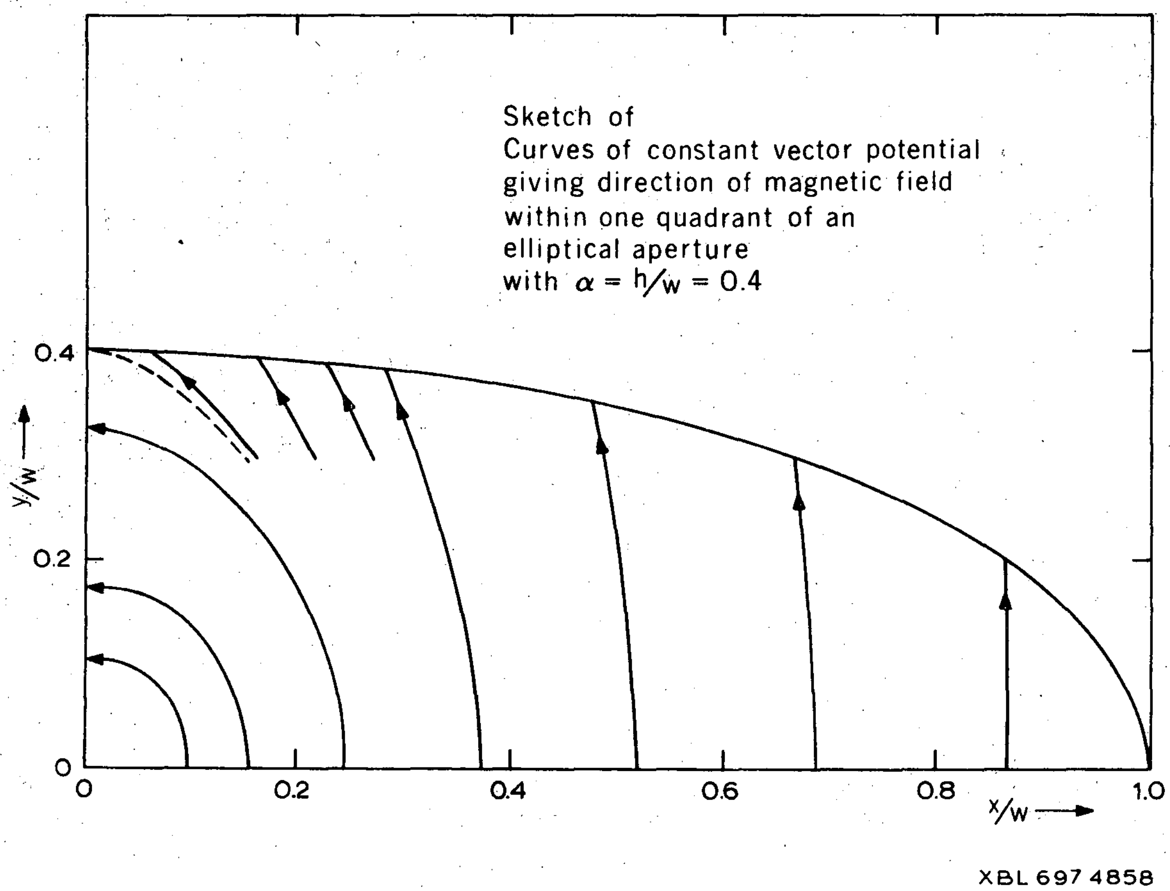
Sketch of
Curves of constant vector potential
giving direction of magnetic field
within one quadrant of an
elliptical aperture
with $\alpha = h/w = 0.4$
0.4
0.2
0
$y/w$
0
0.2
0.4
0.6
0.8
1.0
$x/w$
XBL 697 4858

Fig. 1

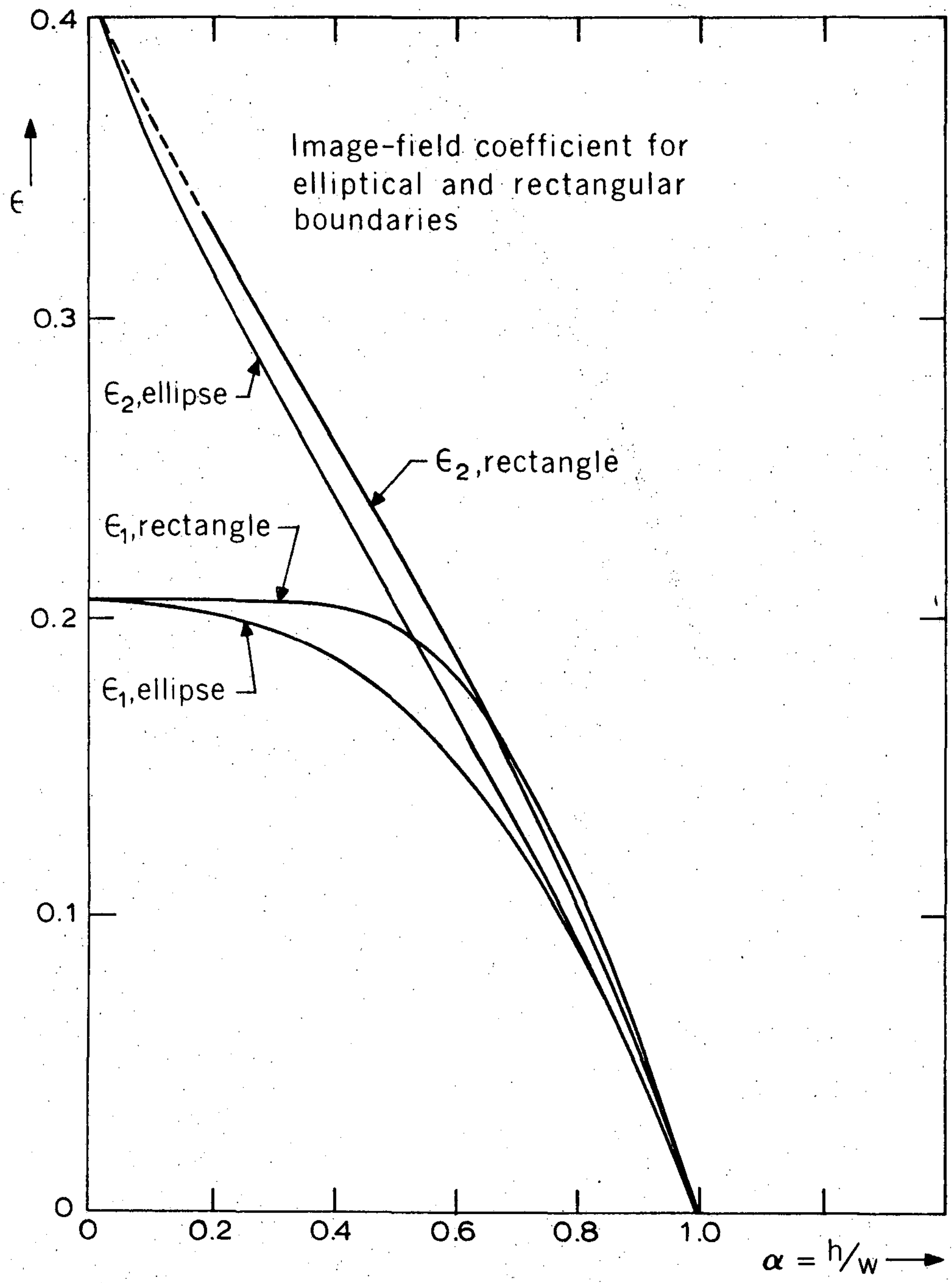


XBL 697-4837

Fig. 2

TECHNICAL INFORMATION DIVISION
LAWRENCE RADIATION LABORATORY
UNIVERSITY OF CALIFORNIA
BERKELEY, CALIFORNIA 94720